Mechatronics, Electrical Power, and Vehicular Technology 05 (2014) 99-106

Mechatronics, Electrical Power, and Vehicular Technology

e-ISSN:2088-6985
p-ISSN: 2087-3379
Accreditation Number: 432/Akred-LIPI/P2MI-LIPI/04/2012

www.mevjournal.com

ADHESION DETECTION ANALYSIS BY MODELING RAIL WHEEL SET DYNAMICS UNDER THE ASSUMPTION OF CONSTANT CREEP COEFFICIENT

Zulfiqar Ali Soomro [a, *]
[a] Directorate of Post-graduate Studies, Mehran University of Engg & Tech
Jamshoro (Sindh) PAKISTAN

Received 21August 2014; received in revised form 14 November 2014; accepted 14 November 2014
Published online 24 December 2014

Abstract

Adhesion level control plays significant role in order to keep smooth running of a train. To design a proper adhesion controller, adhesion dynamics needs to be analyzed. In this paper adhesion is analyzed by modeling rail wheelset dynamics under the assumption of constant creep coefficient. Equations of creepage and creep forces were derived in longitudinal, lateral and angular directions. Numerical simulation was conducted under assumption of constant creep coefficient. The creep coefficient was obtained by applying Coulomb's law of friction. From the simulation results it can be concluded that adhesion level for suitable dynamic model determination depends on assumption of creep analysis to avoid slip or derailment of rail wheelset.

Keywords: adhesion, rail wheel set, creep coefficient, longitudinal, lateral.

I. INTRODUCTION

The study of railway vehicle braking is important to investigate in-train forces, ride comfort, safe operation, braking distance and time, and vehicle speed. Modeling the longitudinal dynamics of trains is important to understand the behavior of rail vehicles while in operation.

This can also help with better understanding the effects of braking forces and other forces and moments that resist the forward motion of the train. Improving dynamic braking forces result in shorter train stopping distance [1-3]. Train speed control and train braking estimations are required to prevent train accidents. PTC is a GPS-based technology that is designed to prevent train collisions and derailments, and to control train movements along the track.

PTC requires understanding the longitudinal train dynamics while operating on the railway network [2, 4]. The interaction forces between the wheel and the rail have a significant effect on the dynamic behavior of the railway vehicle. Adhesion, creep, and wear have significant importance on the railway vehicle dynamics. The adhesion relies upon the environmental conditions and rough surfaces. Creep forces depend upon the wheel dimensions and the rail profile, as well as the materials of the wheel and the rail. In order to calculate the creep forces, wheel/rail contact mechanics must be studied [5].

Polach found that large creep forces mainly occur in the longitudinal direction at the time of traction or braking [6]. Measurements were modeled for five types of locomotives under different weather and wheel/rail conditions [7]. Also, adhesion tests under various speeds and contamination conditions were carried out using a full-scale roller rig in [8].

The results conclude that the adhesion coefficient has high values for dry and clean surfaces and does not change much for all ranges of speeds. It also has low values for oil contamination conditions and does not change much for all ranges of speeds.

The longitudinal rail dynamic model is a two-dimensional model that is used to study the forward motion of the train [9]. A simple model of the longitudinal dynamics of a long freight train was developed [10, 11]. Each group of researchers has focused on longitudinal train dynamics from different perspectives.

* Corresponding Author.Tel: +92-304-0298529
E-mail: zulfiqarali_s@yahoo.com

© 2014 RCEPM - LIPI All rights reserved
doi: 10.14203/j.mev.2014.v5.99-106

The study of the longitudinal train model leads the better concept of the effects upon various conditions and different retardation of the forces which act upon the train dynamics. The behavior of the longitudinal train dynamics is analyzed upon applicationof control design.

A railcar model was developed to study wagon body pitch, derailment, and wheelset skid during braking [12]. This model showed that suddenly applying large braking or traction forces can cause wheel skid. Also, it is mentioned in the study that track defects play an important role in increasing pitch.

The longitudinal dynamic behavior of a train is a function of brake forces and track geometry. Wheel rail interaction forces consist of propulsion resistance and railcar connection. A multibody formulation of the train longitudinal dynamics results in a set of differential equations for each carbody, truck and wheelset. When considering train dynamics, most researchers ignore the vertical and lateral movements, as well as the suspension forces. References [13, 14] extended its application to a more general case.

At the Delft University, Kalker performed his studies applying the limitations as low as possible, conceiving an elliptical contact area with the simultaneous presence of the creepage λx (longitudinal), λy (lateral) and $\lambda\psi$ (spin) [15, 16]. So many theories and algorithms invented procedure as the knowledge based foundation of the modern rail wheelset contact theories [17]. In this paper, creep force analysis is discussed and simulated for dynamic modeling of train for detection of adhesion level to avoid slip.

II. Dynamics of Rail WheelSet

Kalker suggested that the motion is a rigid body motion in the plane of rail wheel contact, i.e., the common tangential plane of wheel and rail, and that the velocity corresponding to this motion is the translational and a rotational about the common normal at the centre of the contact area, which is taken about the z axis [16]. In general, the wheel and rail surfaces can be pressed against each other tangentially displaced and rotated [18].

A. Creep Forces on Wheel Set

The kinematic representation of the wheelset (Klingel formula) has, for a long time been used to explain the sinusoidal behavior of a free wheelset, but the situation is different under a real vehicle. The real wheelset is strongly linked to the vehicle through flexible suspension elements, and these links creates significant forces when the wheelset is entering a curve or running on a real track with irregularities.

The suspension forces find their reaction forces (normal and tangent) at the rail – wheel contact interface, where the tangent components or creep forces are related to the relative speed between the two bodies (creepages). In the contact coordinate systems, the forces are denoted, 'N' for the normal forces, 'F_x' for the longitudinal creep force, 'F_y' for the lateral creep force in the contact plane [18, 19].

In Figure 1, the inner and outer diameters (D_o and D_r) are shown along with concity γ, and spin moment M_z is shown with prescribed creep forces.

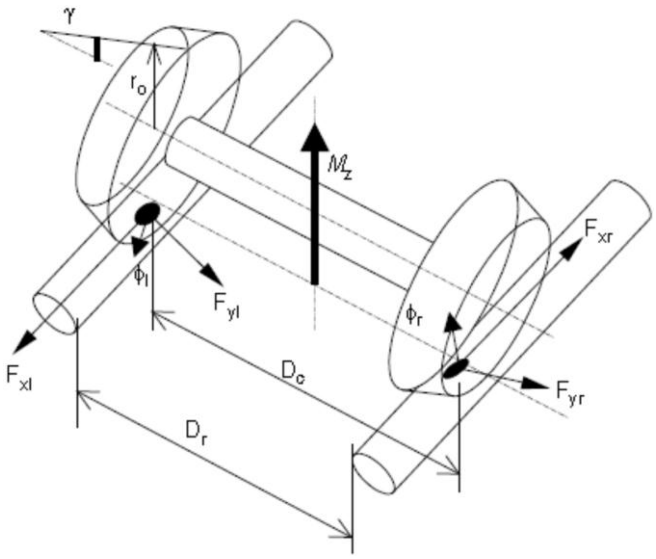

Figure 1.Creep forces and geometry of wheelset

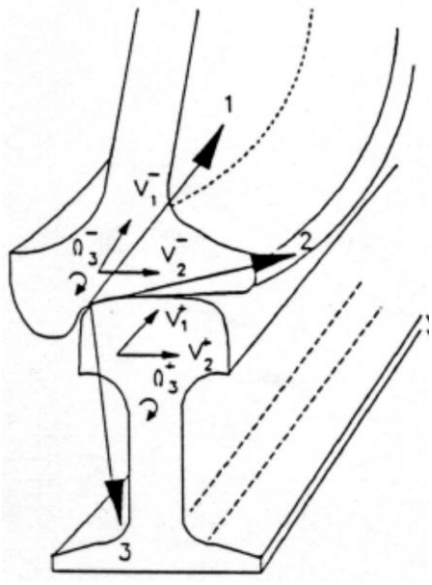

Figure 2. Velocity analysis acting upon wheel and track

B. Velocities and Creepages

Figure 2 shows parameters which are used to analyze relative motions and creepages between wheel and track.

1) Longitudinal Creepage

The wheel profile is conned then longitudinal creep arises when there is a difference in the rolling radii of the two wheels of the wheelset. The longitudinal creepage is defined as follows [20]:

$$\lambda_x = \frac{v^{-1}{}_1 - v^{+1}{}_1}{v} \quad (1)$$

where v_1^{-1}, v_1^{+1}, and v represent forward velocity of wheel, forward velocity of rail, and pure rolling forward velocity, respectively.

2) *Lateral Creepage*

It is defined as the quotient between the lateral components of the relative velocity of the contact points i.e. the lateral slip velocity and the wheel forward velocity. The lateral creepage has a significant effect upon the rails corrugations caused by the lateral creepage forces. Furthermore, the stick-slip phenomenon can be supposed to be induced between a resultant of mainly lateral and longitudinal creepage force.

$$\lambda_y = \frac{v^{-1}{}_2 - v^{+1}{}_2}{v} \quad (2)$$

where v_2^{-1} and v_2^{+1} represent lateral velocity of wheel and lateral velocity of rail, respectively.

3) Spin Creepage

The spin creepage is due to the component of the relative angular velocity of the two bodies normal to the contact surfaces. Generally speaking, the angular velocity of a wheel relative to the rail can be ecomposed into three components; one of them is perpendicular to the contact plane, while the other two are tangent to the plane of contact. However pure rolling occurred when the rolling occurs without sliding or spin [21].

$$\lambda_\Psi = \frac{\Omega_3{}^- - \Omega^+{}_3}{v} \quad (3)$$

where Ω_3^{-1} and Ω_3^{+1} represent forward velocity of wheel and forward velocity of rail, respectively.

Two tangential velocities along x and y axes called rolling velocity. The x-velocity contains the rolling velocity of the vehicle, to which is added some perturbing motions, while the y-velocity contains only perturbations. We can assume that the x component is much larger than the y.

A displacement parallel to the z axes given by δ such displacement is called compression if $\delta < 0$, and loss of contact if $\delta > 0$ [17]. One rotation around the z axis is angular velocity about z. The difference between them is called spin. The spin, divided by the rolling velocity is called spin creepage.

The Longitudinal creepage can confers through the difference in the effective rolling radii of the wheels, left and right, due to the conicity, through acceleration or braking couples and through the rotation of the yaw angle by which the left wheel moves with a different velocity over the rail than the right wheel.

C. Creep Modeling upon Left Rail Wheel

Angular left wheel velocity W_L and forward left wheel velocity v are given by $W_L = v/(r_L + r_o)$ and $v = W_L * r_o$ where r_L denotes inner radius of left wheel.

The concerned velocities in longitudinal, lateral and spin are as follows. Longitudinal creepage of left wheel:

$$\lambda_{xL} = [(r_o * w_L - v)/v] \quad (4)$$

Lateral velocity is given by $\dot{y} = v * \Psi$, where $\Psi = 0.9250\,\text{rad}$ (constant value for spin wheel). Lateral creepage of left wheel:

$$\lambda_{yL} = (\dot{y}/v) - \Psi \quad (5)$$

Yaw (spin) velocity of left wheel:

$$\dot{\psi}_L = W_L / v \quad (6)$$

The longitudinal creep force on left wheel is:

$$F_{xL} = f_{11}\lambda_{xL} \quad (7)$$

The lateral creep force on left wheel is:

$$F_{yL} = f_{22}\lambda_{yL} \quad (8)$$

The spin moment creep force on right/left wheel is:

$$F_{\Psi L} = f_{23}\lambda_{\Psi L} \quad (9)$$

D. Creep Modeling uponRight Rail Wheel

Angular right wheel velocity W_R and forward rightwheel velocity v are given by $W_R = v/(r_R + r_o)$ and $v = W_R * r_o$ where r_R denotes inner right wheel radius.

Longitudinal creepage of right wheel is:

$$\lambda_{xR} = [(r_o * w_R - v)/v] \quad (10)$$

Lateral velocity is given by $\dot{y} = v * \Psi$, where $\Psi = 0.9250\,\text{rad}$.

Lateral creepage of right wheel equals to the lateral creep of left wheel:

$$\lambda_{yR} = (\dot{y}/v) - \Psi \quad (11)$$

Yaw (spin) velocity of right wheel:

$$\dot{\psi}_R = W_R / v \quad (12)$$

Total longitudinal creepage:

$$\lambda_x = \lambda_{xL} + \lambda_{xR} \quad (13)$$

Total lateral creepage (λ_L):

$$\lambda_y = \lambda_{yL} + \lambda_{yR} \quad (14)$$

Total spin (yaw) creepage:

$$\lambda_\Psi = \dot{\Psi}_L + \dot{\Psi}_R \quad (15)$$

Thus combining all the above creepages we get total creepage of rail wheelset as below:

$$\lambda = \sqrt{\lambda_x^2 + \lambda_y^2 + \lambda_\Psi} \quad (16)$$

The longitudinal creep force on right wheel is:

$$F_{xR} = f_{11}\lambda_{xR} \quad (17)$$

The lateral creep force on right wheel is:

$$F_{yR} = f_{22}\lambda_{yR} \quad (18)$$

The spin moment creep force on right wheel is:

$$F_{\Psi R} = f_{23}\lambda_{\Psi R} \quad (19)$$

Total creep forces:

$$F = F_x + F_y + F_\Psi \quad (20)$$

where f_{11}, f_{22} and f_{23} are the creep coefficient of longitudinal, lateral and spin moment.

III. Application of Coulomb's Law

Coulomb's law holds in limited usage and range with approximate to detect coefficients of friction of sliding [13]. It determines the angle of friction and repose by comparing tangential and normal forces. It describes the following relations:

$$f_n = m.g.\cos\alpha \quad (21)$$

$$f_t = m.g.\sin\alpha \quad (22)$$

It states that:

$$f_t = \mu.f_n \quad (23)$$

Means the body is in rest that there is no any slip. And if $f_t \le \mu.f_n$, then there is slip.

Putting values from equations (21 and 22) into equation (23) we get $m.g.\sin\alpha = m.g.\cos\alpha$ hence $\alpha = \tan^{-1}\mu$ .Thus $\mu = \tan(\alpha)$, it further explains that $f_t = \mu.f_n$ means left sliding and if $f_t = -\mu.f_n$ means right slidingon motion. Where f_t is total tangential force, f_n is normal force and $W = m.g$.

IV. Results and Discussion

Since the friction between rail track and wheelset is very complicated and difficult problem, here we have focused on simple approximation to apply Coulomb's law of sliding friction with known coefficient of friction or creep co-efficient.

In the real world, this assumption is applicable hence we can sustain to walk based on the second law of motion. If there would have not been friction, everything would have been slippery. Mathematical dynamics are simulated by using Matlab®.

The results are plotted in the following graphs. Here longitudinal, lateral and yaw velocities are applied upon each wheel of rail wheelset to check their behavior over dynamics and running for rail vehicle on track. Similarly concerned creep forces in major directions are acted upon each

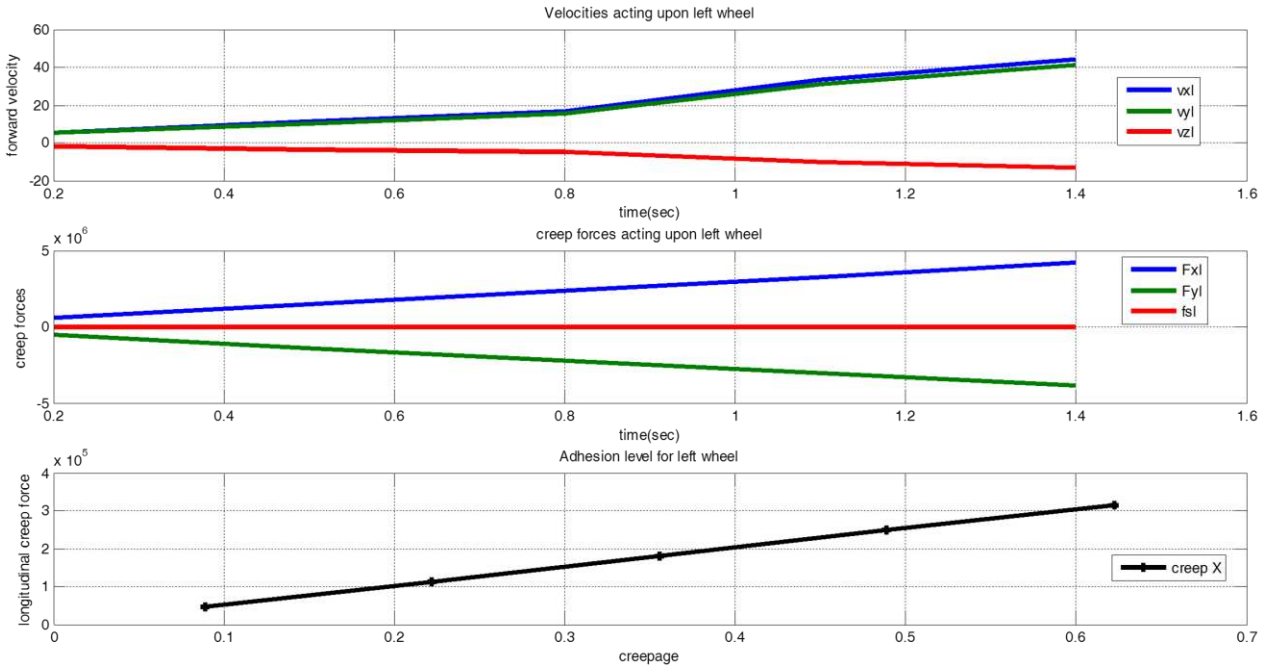

Figure 3. Action of velocities, creep forces and detection of adhesion on left wheel

wheelset. Thus through these analysis, the level of adhesion is detected to avoid slip from derailment.

In the 1st part of Figure 3, the velocities working in three directions have been shown. The blue line representing velocity in longitudinal direction starts above 0 with a little rise upward to end at 40 m/s. Similarly the green line denoting velocity in lateral direction starts from same destination along with and a little bit lower than longitudinal line to end at same stop. Whereas the red line denoting the yaw velocity starts from 0 and falls gradually lower than 0 to end at -18 rad/s in 1.4 seconds, like the previous lines of longitudinal and lateral velocities.

In the 2nd part of Figure 3, the creep forces working in mentioned three directions have been shown. The blue line representing force in longitudinal direction starts above 0 with a little rise upward linearly to end at 4e+6 mN. Similarly green line denotes force in lateral direction falls linearly from same destination lower than longitudinal line to ends below 0 in 1.4 seconds. Whereas red line denotes the yaw force starting from 0 and falls gradually lower than 0 to end at nearly -4.8 mN in 1.4 seconds. Similarly spin moment start from 0 in straight line linearly without any change which reflects the idea that yaw rate are the same among longitudinal and lateral velocities.

In the 3rd part of Figure 3, total creepage is compared with longitudinal force of left to detect the adhesion level to protect from slippage. Here the curve starts from 0 to travel linearly in straight path up to 3e+6 mm/s in 0.63 seconds. This denotes that adhesion level is increased to control slip. This straight line represents maximal Coulomb's law for friction in contact surfaces.

In the 1st part of Figure 4, the velocities working in three directions have been shown. The blue line representing velocity in longitudinal direction starts above 0 with a little rise upward to end at 100 m/s. Similarly the green line denotes velocity in lateral direction starts from same destination along with a little bit lower than longitudinal line to end at same stop at 1.4 seconds.

Whereas red line denotes the yaw velocity starts from 0 and falls gradually lower than 0 to end at -45 rad/sec in 1.4 seconds, like previous lines of longitudinal and lateral velocities. In the 2nd part of Figure 4, the creep forces working in mentioned three directions have been shown.

The blue line representing force in longitudinal direction starts above 0 with a little rise upward linearly to end at 4 N in 1.4 seconds. Similarly green line denotes force in lateral direction falls linearly from same destination lower than longitudinal line to ends below 0 in 1.4 seconds. Whereas red line denotes the yaw velocity starts from 0 and falls gradually lower than 0 to end at nearly -4.8 N in 1.4 seconds. Similarly spin moment start from 0 in straight line linearly without any change which reflects

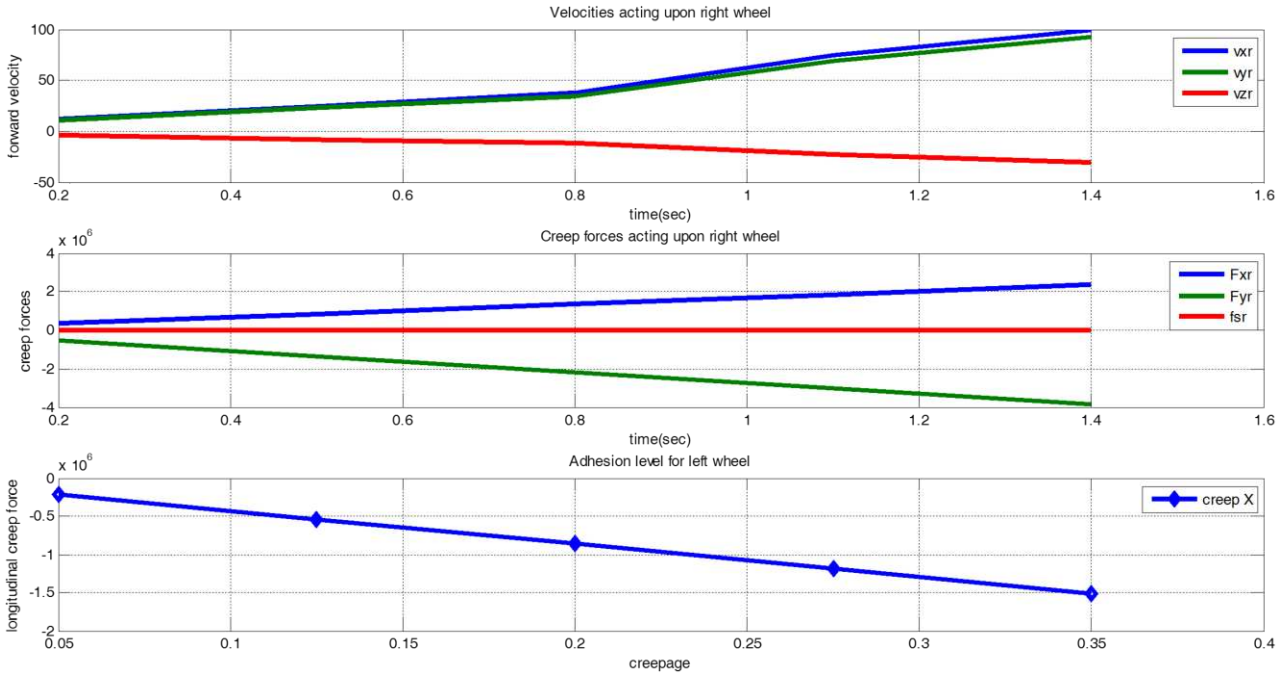

Figure 4. Action of velocities, creep forces and detection of adhesion on right wheel

the idea that yaw rate are the same among longitudinal and lateral velocities.

In the 3rd part of Figure 4, total creepage is compared with longitudinal force of right wheel to detect the adhesion level to protect from slippage. Here the curve starts from 0 to travel linearly in straight path up to -2e+6 mm/s in 0.35 seconds. This denotes that adhesion level is increased to control slip. This straight line represents maximal Coulomb's law for friction in contact surfaces.

In the 3rd part of Figure 5, total creepage is compared with spin moment force of wheel set to detect the adhesion level to protect from slippage.

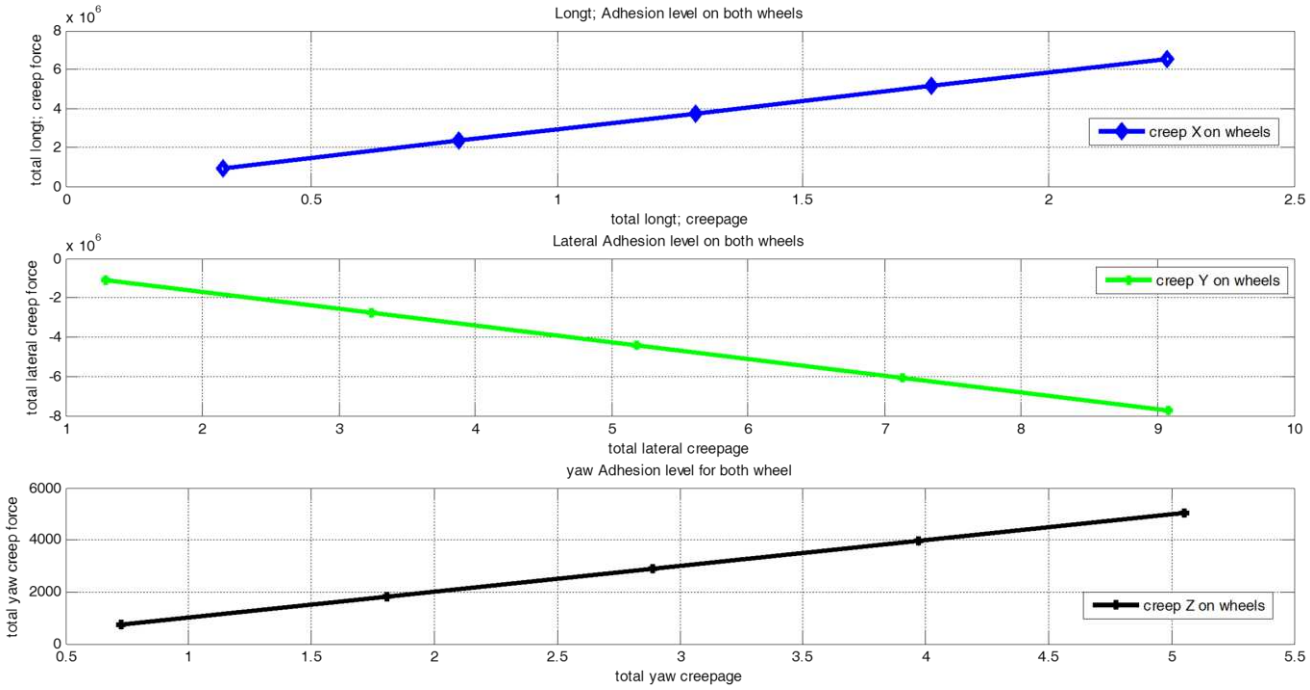

Figure 5. Behavior of total 3D creep forces and creepage to detect adhesion on wheelset

Here the black line representing adhesion level starts from 0 to 5,000 mN of yaw forces linearly in straight path with vertical to 5.1 N total creepage horizontally.

This denotes that when spin force rises with increase of total creepage, hence adhesion level is increased to control slip. This straight line represents maximal Coulomb's law for friction in contact rough surfaces.

Here μ = 0.15 and f_t = -8.5622e+005. By substituting into equation (23) and after re-arrangement we get $f_n = f_t/\mu$ = -5.7082e+006 which is greater than f_t but $\mu.f_n$ is equal to f_t. It demonstrates that there is small ratio of overall slip.

To determine entire adhesion for verifying slip ratio this model is good enough to explore relative problems, and perform smoothly. From whole discussion it can be observed that this designed model helps to detect adhesion level to control precautionary steps from incident of slip from huge accidents. This dynamic model paves path to invent adhesion measuring instrument to avoid slip depending upon creep forces and velocity analysis

V. CONCLUSION

In above analysis, the railway wheelset model was taken to enumerate its concerned dynamics to calculate the creep forces and creepage acting upon it. The velocities of wheelset and rail track were assumed and discussed on each rail wheel to compute the creep forces in main directions i.e. longitudinal, lateral and spin. Thus total creep forces of these three dimensions were compared with total creepage of these directions to identify the level of adhesion for escaping from slip to avoid derailment of rail vehicle. Coulomb's law for sliding friction was used to verify the validation of the linear model. The modeling and simulation by Matlab® is well sufficient to detect the adhesion manually too.

REFERENCES

[1] H. Ahmad and M. Ahmadian, "Train braking distance estimation under different operating conditions," in *ASME 2011 Rail Transportation Division Fall Technical Conference*, Minneapolis, Minnesota, USA, 2011.

[2] H. Ahmad and M. Ahmadian, "Model reference adaptive control of train dynamic braking," in *ASME 2012 Joint Rail Conference*, Philadelphia, Pennsylvania, USA, 2012.

[3] (2013, July). *Federal Railroad Administration*. Available: http://www.fra.dot.gov

[4] (2013). *Association of American Railroads*. Available: www.aar.org

[5] V. K. Garg and R. V. Dukkipati, *Dynamics of railway vehicle systems*: Academic Press, 1984.

[6] O. Polach, "A fast wheel-rail forces calculation computer," *Veh. Syst. Dyn. Suppl.,* vol. 33, pp. 728-739, 1999.

[7] W. Zhang*, et al.*, "Wheel/rail adhesion and analysis by using full scale roller rig," *Wear,* vol. 253, pp. 82-88, 2002.

[8] L. Pugi*, et al.*, "Modelling the longitudinal dynamics of long freight trains during the braking phase," in *12th IFToMM World Congress*, France, 2007.

[9] Z. Zhang and M. Dhanasekar, "Dynamics of railway wagons subjected to braking/traction torque," *Vehicle System Dynamics,* vol. 47, pp. 285-307, 2009/03/01 2009.

[10] S. Iwnicki and A. H. Wickens, "Validation of matlab vehicle simulation using a scaled test rig," *Vehicle System Dynamics,* vol. 30, pp. 257-270, 1998.

[11] S. Iwnicki, *Handbook of railway vehicle dynamics*: Taylor & Francis, 2006.

[12] A. A. Shabana*, et al.*, "A multi-body system approach for finite-element modelling of rail flexibility in railroad vehicle applications," *Proceedings of the Institution of Mechanical Engineers, Part K: Journal of Multi-body Dynamics,* vol. 222, pp. 1-15, March 1, 2008 2008.

[13] J. Pombo, "A multibody methodologyfor railway dynamics applications," PhD Thesis, Instituto Superior T´ecnico, Universidad T´ecnica de Lisboa, 2004.

[14] A. Shabana and J. Sany, "A survey of rail vehicle track simulations and flexible multibody dynamics," *Nonlinear Dynamics,* vol. 26, pp. 179-212, 2001/10/01 2001.

[15] J. J. Kalker, "A Strip theory for rolling with slip and spin," in *Proceedings Kon. Ned. Akad. Van Wetenshappen*, 1967.

[16] J. J. Kalker, *Three-dimensional elastic bodies in rolling contact*: Dordrecht: Kluwer Academic Publishers, 1990.

[17] M. Ishida*, et al.*, "The effect of lateral creepage force on rail corrugation on low rail at sharp curves," *Wear,* vol. 253, pp. 172-177, 2002.

[18] I. Y. Shevtsov, *et al.*, "Optimal design of wheel profile for railway vehicles," *Wear,* vol. 258, pp. 1022-1030, 2005.

[19] I. Y. Shevtsov, *et al.*, "Design of railway wheel profile taking into account rolling contact fatigue and wear," in *7th International Conference on Contact Mechanics and Wear of Rail/Wheel Systems (CM2006)*, Brisbane, Australia, 2006, pp. 667-674.

[20] P. Gaspar, *et al.*, "Observer based estimation of the wheel-rail friction coefficient," in *2006 IEEE International Conference on Control Applications*, Munich, Germany, 2006, pp. 1043-1048.

[21] Y. Zhao, *et al.*, "Estimation of the friction coefficient between wheel and rail surface using traction motor behaviour," *Journal of Physics: Conference Series,* vol. 364, p. 012004, 2012.